08,04,16

Separate observation of the electronic Mott transition and the structural Peierls transition in vanadium dioxide

© A.V. Ilyinsky[1], A.A. Kononov[2], E.B. Shadrin[1]

[1] Ioffe Institute,
St. Petersburg, Russia
[2] Herzen Russian State Pedagogical University,
St. Petersburg, Russia

E-mail: shadr.solid@mail.ioffe.ru

Received March 7, 2025
Revised March 10, 2025
Accepted March 10, 2025

It has been shown that temperature changes in the newly discovered fine structure of the dielectric spectra of nanocrystalline vanadium dioxide films provide exclusive experimental evidence for the complex Mott-Peierls nature of the complex semiconductor-metal phase transition in VO_2 films.

Keywords: dielectric spectroscopy, vanadium dioxide, semiconductor-metal phase transition, VO_2 films, specific conductivity.

DOI: 10.61011/PSS.2025.04.61272.71-25

1. Introduction

Vanadium dioxide is a strongly correlated material [1–4] that exhibits a temperature-extended narrowing of the forbidden band width E_g of the semiconductor phase as a result of a thermal increase in the concentration of free equilibrium electrons in the conduction band. This process is known as the Mott semiconductor-metal phase transition (PT) [2]. The quantum-mechanical description of the Mott PT is based on an additional account, along with the electron-nuclear interaction, of the inter-electron interaction, thus reducing to the solution of a multiparticle problem. This problem is solved by introducing an additional energy term describing the inter-electron interaction into the Hamiltonian. The numerical value of this kind of additional energy, called the correlation energy [3], is chosen by matching the results of calculations with measurements. The correlation energy is also introduced into the electron energy distribution function, which leads to the replacement of the Fermi distribution by the Migdal distribution [4].

The complex nature of PT in vanadium dioxide is manifested in the fact that the Mott electron transition in this material is followed by the Peierls structural transition from a low-symmetric crystal phase of monoclinic symmetry to a high-symmetric crystal phase of tetragonal symmetry takes place [5]. Historically, this conclusion was reached as early as 2000 when it was shown in Ref. [5] that (quote) „semiconductor-metal PT in vanadium dioxide behaves like an electronic PT in that its initial stage is the rearrangement of the electronic subsystem of the material, and the inevitable changes in the crystal lattice are secondary in nature and are a stage in the process of transition of the sample from the semiconductor state to the metallic state, immediately following the excitation of the electronic subsystem of the material". A number of new papers [6–10] have been presented since the above publication in which this kind of ideas about the complex nature have been confirmed, refined, and extended. For instance, the electronic component of the PT was experimentally identified in Ref. [7]. This identification was based on the fact that the structural Peierls PT has hysteresis, whereas the Mott electronic transition does not. It was found in Ref. [9] that the Mott PT in vanadium dioxide occurs in femtosecond time, and it was shown in Ref. [10] that the optical properties of such a unique system as a photonic crystal can be controlled using VO_2 synthesized in the pores of a photonic crystal, and such control of the electronic PT parameters is also performed on a femtosecond time interval [11]. New and unique results have been obtained recently on the way to expanding the range of vanadium compounds studied by dielectric spectroscopy methods [12–14]. In particular, the complex Mott-Peierls character of the PT was established in a whole series of strongly correlated compounds such as VO, VO_2, V_2O_3, V_2O_5, which are part of the nomenclature of oxides of the Magnelli series. It has been shown that as the oxidation degree of atom V increases, the numerical value of the metallic conductivity value of the high-temperature phase of the above oxides drops naturally and simultaneously the temperature of the PT of the material to the metallic state increases.

The aim of this paper is to demonstrate new exclusive possibilities of dielectric spectroscopy as a method to investigate the nature of phase transformations. These kinds of opportunities are based on the unique advantage of this method, which is based on the fact that the PT parameters, which cannot be studied by other experimental methods, are directly manifested in dielectric spectra (DS). In particular, the analysis of DS using the concept of equivalent electrical circuits allows us to determine the

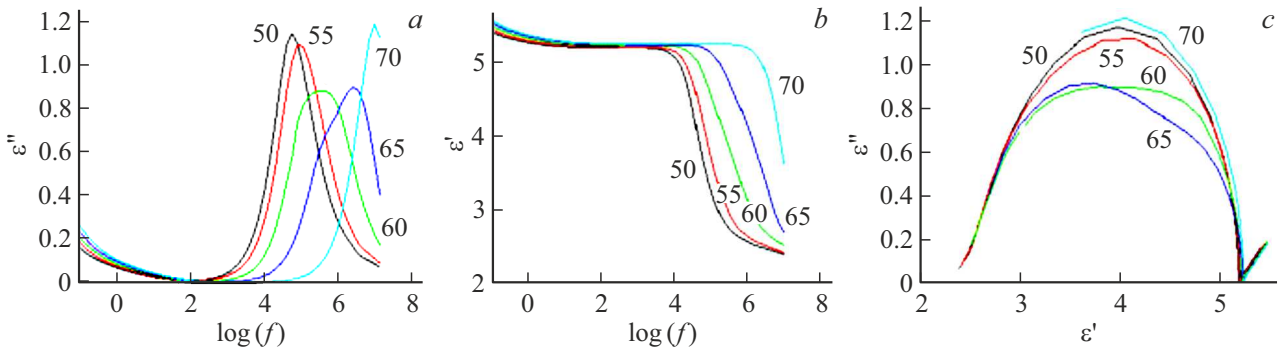

Figure 1. Experimentally measured frequency dependences a — $\varepsilon''(f)$, b — $\varepsilon'(f)$ and c — Cole-Cole diagram in the temperature region 50−70 °C from Ref. [12].

value of the specific conductivity of each particular type of nanocrystalline grains by isolating this grain type from the total variety of grain types of the film sample. It also allows to perform quantitative estimates of the concentration ratio of different types of grains and to calculate the ratio of areas occupied on the substrate surface by grains of VO_2 film of different types randomly distributed in the total population of grains. Finally, this method provides an opportunity to experimentally trace the variation of phase transformation parameters in each particular type of grains by monitoring the temperature variation of their DS resonance features.

2. Dielectric spectra and their description

Experimentally measured DS of undoped vanadium dioxide thin films were provided in [12] — see Figure 1. The fundamental interest in these spectra is attributable to the fact that in the semiconductor-metal PT temperature region (50−70 °C), not only a thermal shift of the resonance frequency of the location of the maxima of the DS features, but also a change in the magnitude of the spectral features in the maximum, as well as a change in the shape of these features, is observed when the temperature of the sample is changed. I. e., the fine structure of DS not observed earlier is manifested. Indeed, at $T = 50\,^{\circ}\mathrm{C}$, the imaginary part of the dielectric constant $\varepsilon''(f)$ has a well-defined maximum at frequency $10^{4,5}$ Hz (a), and at the same frequency, the step in the plot of the functional dependence of the real part of dielectric permittivity on frequency $\varepsilon''(f)$ (b) is clearly expressed, and the Cole-Cole diagram $\varepsilon''(\varepsilon')$ is a regular half-circle (c). The DS features shift toward high frequencies with temperature rise. The height of the maximum $\varepsilon''(f)$ decreases, its half-width increases, the frequency interval occupied by the step on the graph $\varepsilon'(f)$ increases in width, and the half-circle $\varepsilon''(\varepsilon')$ acquires an irregular shape (Figure 1). A splitting of the broad maximum $\varepsilon''(f)$ is observed at $T = 65\,^{\circ}\mathrm{C}$ in the form of the appearance of a structure in the form of a frequency doublet, and at $T = 70\,^{\circ}\mathrm{C}$ the maximum $\varepsilon''(f)$ at the frequency $f = 10^7$ Hz again becomes narrow and high (Figure 1).

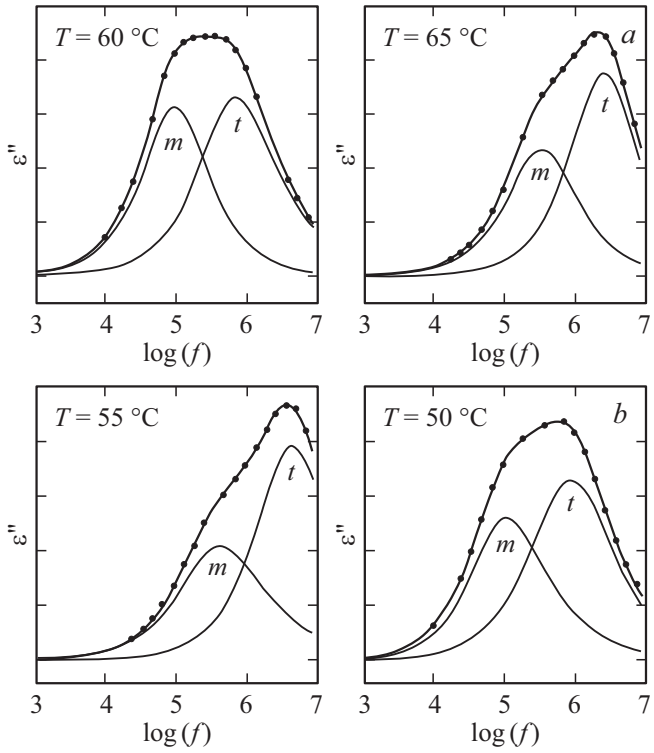

Figure 2. Decomposition of the fine structure of DS features into two components m and t.

The above is well illustrated by the decomposition of the feature $\varepsilon''(f)$ into two Gaussian components, labeled m and t, shown in Figure 2.

It follows from the above that, in order to describe the fine structure of the spectrum, Debye's formula should be complicated by introducing the function $G(\tau)$ of the distribution of relaxants by relaxation times:

$$\varepsilon^*(\omega) = \varepsilon_\infty + \Delta\varepsilon \int_0^\infty \frac{G(\tau)}{1 + i\omega\tau}\, d\tau. \qquad (1)$$

By appropriate selection of the relaxation times of the $G(\tau)$ function, represented, for example, as two functions

similar to the δ-function, or two Havriliak-Negami [15] functions, a good agreement of the calculation results with the measurement results can be achieved. However, progress in this direction seems to be unpromising due to the lack of a clear relationship between the dielectric spectrometer cell parameters and the parameters of the studied sample.

An alternative and at the same time more definitely reflecting the physical picture of the phenomena the possibility to describe DS is the use of equivalent electrical circuits, adequately corresponding to the studied sample. The relatively simple equivalent circuit shown in Figure 3, *a* gives a good result. Here C_s is the capacitance of the insulating mica substrate on which the film VO_2 was synthesized, characterized by the capacitance C and resistance R.

Calculations in Ref. [13] performed using this scheme yield function plots of $\varepsilon'(f)$, $\varepsilon''(f)$, and $\varepsilon''(\varepsilon')$, within the accuracy of the experiment, matching the plots of Figure 1, but not describing the fine structure of DS.

Thus the symbols of the Debye (1) formula have the following physical meaning:
$G(\tau)$ — δ-function, $\varepsilon_o = \varepsilon' = \frac{C_s I}{C_0}$ (corresponding to the limit $\varepsilon'(\omega)$ at $\omega \to 0$), C_s is the substrate capacitance, C_o is the capacitance of the empty cell of the dielectric spectrometer, i. e. ε_o represents the dielectric constant of the insulating substrate alone, since the thermally generated influx of free electrons ($R = \text{const}$) completely displaces the constant (in the limit $\omega \to 0$) probing electric field from the semiconductor film into the dielectric substrate at the low-frequency boundary of the frequency range of variation of the probing electric field used for the study.

At the same time we have the following expression at the high-frequency boundary of this range

$$\varepsilon_\infty = \varepsilon' = \frac{CIC_sI}{(CI + C_sI)C_0}$$

(corresponding to the limit $\varepsilon'(\omega)$ with $\omega \to \infty$). Thus, at the high-frequency limit of the frequency range, the real part of the complex permittivity is a combination of series-connected capacitances (C is the semiconductor film capacitance, C_s is the substrate capacitance). That is, the high-frequency limit of the frequency range corresponds to those conditions under which the charge carriers in a thin film of semiconductor „do not have time to move“ when a high-frequency probing external field is applied, not being able to shield it even to a small extent.

We would like to remind that $\tau_D = \tau_m = \varepsilon\varepsilon_o/\sigma$ is the Maxwell relaxation time, σ is the specific conductivity of the semiconductor film VO_2. Indeed, resonance in the equivalent circuit is achieved at frequency f_0 [13]:

$$f_0 = \frac{1}{2\pi RICI\sqrt{\frac{C_sI}{CI} + 1}},$$

and after conversion, we have:

$$1/\omega_o = 1/(2\pi f_o) = RC(C_s/C + 1)^{1/2}$$

$$= \rho\varepsilon\varepsilon_0[\varepsilon_s d/(\varepsilon D) + 1]^{1/2} = \varepsilon\varepsilon_0/\sigma = \tau_m = \tau_D.$$

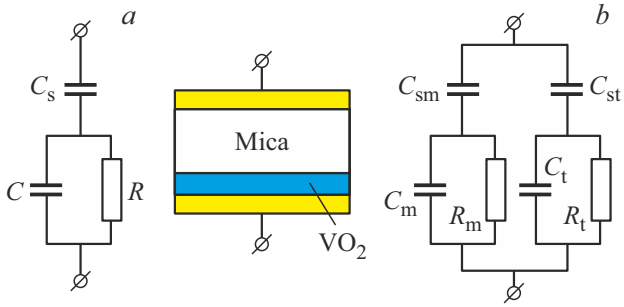

Figure 3. One-loop (a) and two-loop (b) equivalent circuits of a dielectric spectrometer cell with a sample in the form of VO_2 film synthesized on the surface of a mica plate.

Along with this, the value of $\varepsilon''(\omega_o)$ at the resonance frequency ($\omega_o\tau_D = 1$) is:

$$\varepsilon'' = \Delta\varepsilon/2 \cdot (\varepsilon_o - \varepsilon_\infty)/2$$

and does not depend on the conductivity of the film material. In our case (Figure 2) $\varepsilon''(\omega_o) = 1.5$. The question naturally arises what the value $\varepsilon''(\omega_o)$ at the resonance frequency can depend on if it is determined by only two constants: ε_o and ε_∞? To answer this question, let us express the value of $\varepsilon''(\omega_o)$ through the elements of the single-loop equivalent circuit (Figure 3, *a*):

$$\varepsilon''(\omega_o) = (\varepsilon_o - \varepsilon_\infty)/2 = C_s^2/[2(C + C_s)C_o]. \qquad (3)$$

The formula (3) shows that the value $\varepsilon''(\omega_o)$ is determined only by the capacitance values and is independent of the film conductivity. From the fact that the numerical values of the capacitances are determined by the degree of overlap of the effective area of the film under study with the electrodes of the dielectric spectrometer cell, it follows that if, for example, only one nanocrystalline grain is synthesized on the insulating substrateVO_2 (hypothetically) with specific conductivity δ, then resonance at frequency $\omega_o = 1/\tau_m$ will occur, but the value $\varepsilon''(\omega_o)$ will be vanishingly small. Obviously, the value of $\varepsilon''(\omega_o)$ will increase as the effective overlap area of the semiconductor film with the electrodes increases with the number of identical grains.

If the semiconductor film consists of two types of grains with specific conductivities δ_m and δ_t, the DSs will have resonant features at the two frequencies ω_m and ω_t. Moreover, the values of $\varepsilon''(\omega_m)$ and $\varepsilon''(\omega_t)$ will be determined by the total areas of all grains of each type regardless of the degree to which they are mixed with each other on the substrate surface. This case is considered quantitatively in Ref. [14] involving a two-loop equivalent circuit (Figure 3, *b*).

Figure 4 shows the DSs calculated using the described scheme. The constants ε_o and ε_∞, expressed through the parameters of the equivalent circuit of Figure 3, *b*, were selected by fitting to the experimental results. In this case, the resonance frequencies ω_m and ω_t are strongly separated in magnitude for better clarity, which leads to a strong

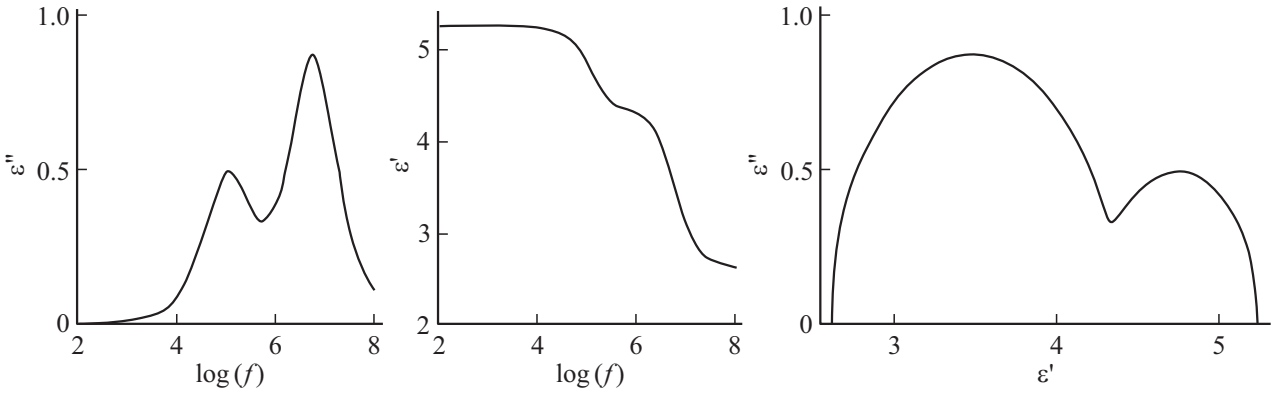

Figure 4. Result of DS calculations using the double-loop scheme $C_o = 38\,\text{pF}$, $\varepsilon_s = 5.25$, $k = 1$, $C_{sm} = 130\,\text{pF}$, $C_m = k \cdot C_{sm}$, $R_m = 10^2\,\Omega$, $C_{st} = \varepsilon_s \cdot C_o - C_{st}$, $C_t = k \cdot C_{st}$, $R_t = 10^4\,\Omega$.

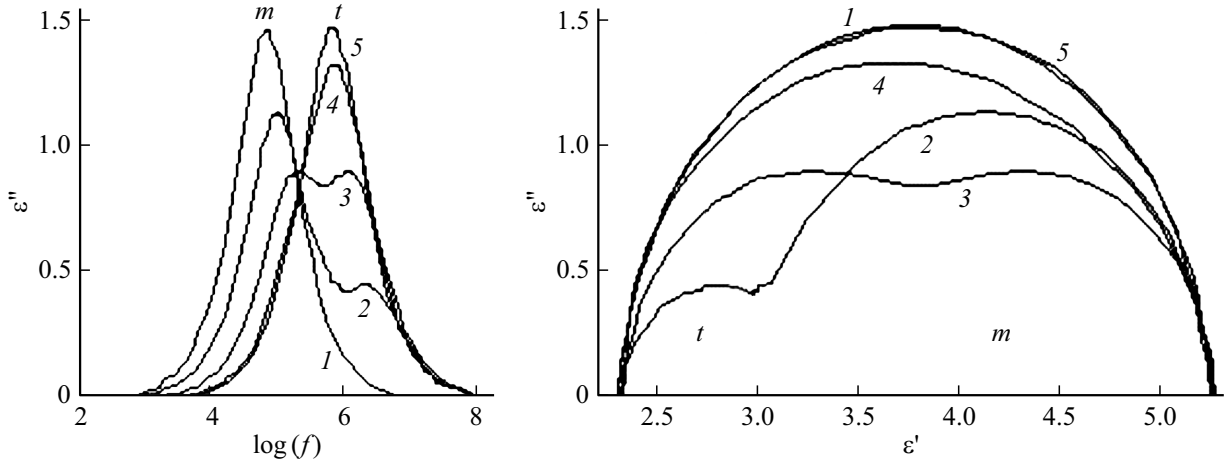

Figure 5. Results of the frequency dependence of $\varepsilon''(f)$ and Cole-Cole diagrams calculated by the double-loop scheme when the ratio between the areas occupied by nanocrystallites of two different **m** and **t**-types is changed: S_m and S_t — 1 and 0 (*1*), 0.75 and 0.25 (*2*). 0.5 and 0.5 (*3*), 0.25 and 0.75 (*4*), 0 and 1 (*5*). ($C_o = 38\,\text{pF}$, $\varepsilon_s = 5.25$, $R_m = 5 \cdot 10^2\,\Omega$, $R_t = 5 \cdot 10^3\,\Omega$, $k = 1$, $C_m = k \cdot C_{sm}$, $C_{st} = \varepsilon_s \cdot C_o - C_{sm}$, $C_t = k \cdot C_{st}$, where $C_{sm} = 200$ (*1*), 150 (*2*), 100 (*3*), 50 (*4*) and 0 pF (*5*)).

separation on the horizontal axis of the features of the functions $\varepsilon''(\omega_m)$ and $\varepsilon''(\omega_t)$.

By converging the numerical values of the resonance frequencies characterizing the position of the DS features, the result of the numerical calculation can be obtained in good agreement with the measurement results (Figure 5).

3. Discussion of results

The temperature region of DS variation considered in this paper represents the region of semiconductor-metal thermal PT realization in VO_2. As mentioned in the introduction, the PT in vanadium dioxide has a complex character, characterized by the fact that the structural Peierls PT is preceded by the electronic Mott transition, which occurs in a wide temperature range up to the contact on the energy scale of the bottom of the conduction band π^* with the ceiling of the valence band d_{bott}. This circumstance initiates a structural Peierlss PT from the monoclinic to the tetragonal crystalline phase. We emphasize that all nanocrystalline grains of vanadium dioxide film have the same specific conductivity at temperatures below the PT temperature regardless of their size. This statement is in good agreement with experiment, since only one resonance feature is observed in DS in the form of a sharp maximum $\varepsilon''(f)$ (acute maximum of the feature $\text{tg}\,\delta(f)$), a well-defined step $\varepsilon'(f)$, and the regular shape of the Cole-Cole diagram half-circle also emphasizes the individual uniqueness of this feature $\varepsilon''(f)$.

Let us demonstrate the concrete manifestation in DS of the very fact of occurrence of the PT by considering a model version of the analysis, in the initial stages of which we will analyze two limiting cases, after which we will merge them.

At the first initial stage of the analysis, let us conventionally assume that there is no structural Peierls PT in nanocrystallites, i. e., only electronic Mott PT is takes place.

The energy levels are located close to each other in π^*-conduction band due to its narrowness in terms of energy. Therefore, a gradual increase of electron concentration

in π^*-conduction band (formed by expansion into the area of the π^*-level of the antibinding molecular orbital (MO) of the bond $V^{4+}-O^{4-}$) in case of a slow increase of temperature ensuring the establishment of the thermodynamic equilibrium leads, according to the conclusions of the molecular orbital theory, to the narrowing of the energy gap between the binding π-MO and antibinding π^*-MO, simultaneously bringing them closer to the vacuum energy level. In the case of VO_2, this leads to a narrowing of the band gap ($E_g = 0.7$ eV), the role of which is played by the energy gap between the empty antibinding π^*-band and the filled lower Hubbard subband d_{bott} [5]. The mechanism of narrowing is determined by electron throwing into the π^*-band from the lower Hubbard subband $3d_{\text{bott}}$, since the role of the binding MO in VO_2 is played by d_{bott}, and, according to the MO method, carrier throwing strongly shifts both binding and antibinding bands towards the vacuum energy level, but shifts with sharply different rates, as it should be in strongly correlated compounds. This difference reduces the energy gap between π^* and d_{bott} that is initially equal in VO_2 0.7 eV [5] because of the large difference in the energy velocity of the bands as they are populated [16].

The high efficiency of the electron throwing itself through the gap of 0.7 eV at $T = 67\,^\circ$C (340 K) is determined by the fact that the electron energy distribution in strongly correlated materials follows the law called, as mentioned above, the Migdal distribution, which replaces the Fermi distribution in strongly correlated materials, and is distinguished by the introduction of the correlation energy into the mathematical expression for the electron energy distribution function. In result of such an throwing, the concentration of free electrons in the π^*band strongly increases with the temperature increase. This leads to a multiple increase of the specific conductivity of the crystalline material in all grains (by orders of magnitude) with the increase of the temperature. In result of such an increase in this hypothetical case of absence of a step-like Peierls PT, one should expect a continuous frequency shift toward high frequencies of the single feature of the DS without changing its magnitude and shape, since the shift is determined by the decrease of the Maxwell relaxation time with increasing conductivity. There is practically no thermal hysteresis of physical parameters of VO_2 nanocrystallites in absolutely pure undoped material. But in reality, the question of temperature hysteresis for the purely electronic Mott transition remains open at this stage of the analysis.

We consider the second limiting case in the next step of the analysis: There is no Mott PT, but there is a structural PT from monoclinic to tetragonal phase, which takes place in different types of film nanocrystallites at different temperatures determined, according to the martensitic ideology, by their average size [17]. In this case, when the temperature increases, the phase transition (PT) from the monoclinic (semiconductor) phase to the tetragonal (metallic) phase is made by a jump (both in temperature and time, since the interface between the monoclinic and tetragonal phases moves along the nanocrystallite at the speed of sound). At the same time, the specific conductivity also jumps up by several orders of magnitude. The numerical value of the increase in specific conductance is the same for all grains regardless of their size. In this case, we should expect a monotonic decrease of the value of $\varepsilon''(f)$ in the low-frequency region (m) with the increase of the temperature and a gradual increase of the value $\varepsilon''(f)$ in the high-frequency region (t), i. e., pumping of intensity between the DS spectral components. This pumping is attributable to the fact that the number of tetragonal metallic grains gradually increases as the temperature increases and the number of monoclinic semiconductor grains decreases.

Figure 5 shows the results of calculation of $\varepsilon''(\omega)$ and $\varepsilon''(\varepsilon')$ by formula (3). The calculations took into account that a decrease in the number of monoclinic grains and a simultaneous increase in the number of tetragonal grains in case of increase of T in the PT region leads to a change in the ratio of areas S_m and S_t ($S_m + S_t = \text{const}$), i. e., to changes in the values of C_m, C_t, and C_{sm}, C_{st}. The graph shows that the low-frequency („semiconductor“) component m prevails at $S_m \gg S_t$ — curve *1*. As the temperature increases, the area S_m gradually decreases and intensity of this component also decreases, and a high-frequency („metallic“) component t appears in the high-frequency region— curves *2–4*. It prevails on the graph in terms of intensity at$T > T_c$ — curve *5*. The calculations assumed that the frequency corresponding to the maximum of the component t was an order of magnitude greater than the frequency of the component m and was assumed to be the same for all grains, since the frequency position of the DS singularities reflects the magnitude of the specific conductivity of the nanocrystallite rather than the absolute value of its conductivity. The presence of two spectral components and the redistribution of intensities between them is also clearly manifested in the thermal evolution of Cole-Cole diagrams. And, of course, for structural PT it is natural to expect the appearance of temperature hysteresis of the frequency position of DS [14].

It seems natural to combine the two cases described above at the final stage of the analysis. Indeed, the experiment shows that with increasing temperature there is a real shift up the frequency scale of the DS singularities (by about three orders of frequency), with the value $\varepsilon''(f)$ initially decreasing and then returning to its previous value. Its shape also changes: a doublet fine structure of this singularity is found at intermediate temperatures 55–65 °C. The height of the singularity of the DS spectrum $\varepsilon''(f)$ decreases and its shape at temperatures of 55–65 °C can be represented as a superposition of two components about an order of magnitude different in frequency. The shape of the singularity changes with the temperature increase due to „pumping“ of intensity from the low-frequency m-component to the high-frequency t-component. Conversely, a „pumping“ of intensity from the high-frequency t-component to the low-frequency m-component takes place with the temperature decrease. All processes are repeated, but in reverse order with a lag of 10 °C. Based on these data, we have plotted the temperature hysteresis

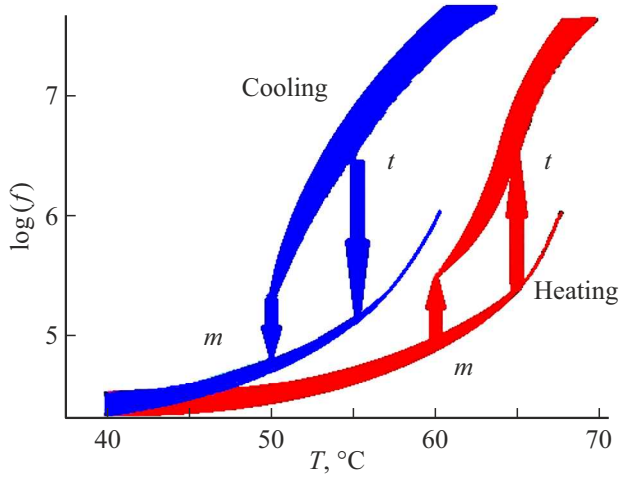

Figure 6. Temperature hysteresis loop of the frequency position $\varepsilon''(f)$ plotted from the data of Figure 1 and Figure 2. Vertical arrows indicate the structural PTs of a part of grains from the monoclinic phase to the tetragonal phase with a step-like increase in the specific conductivity of grains when the film is heated; structural PTs of a part of grains from the tetragonal phase to the monoclinic phase when the film is cooled are also marked

.

loop of the VO_2 film (Figure 6). This figure clearly demonstrates that the heated branch of the loop consists of two components: *m*-monoclinic at low temperatures, which disappears with the increase of temperature, and *t*-tetragonal at high temperatures, which gradually expands with the increase of temperature. The cooling branch of the loop also consists of *m*- and *t*-components at low and high temperatures, respectively. The structural PTs of a portion of grains from one crystalline phase to another are marked by vertical arrows.

4. Conclusion

To summarize, we would like to note that dielectric spectroscopy allows us to experimentally trace qualitatively and quantitatively the details of phase transformations that have a complex nature. The essence of the results obtained in this paper is as follows.

The crystal lattice of all grains of the film have a monoclinic symmetry at low temperatures compared to PT temperatures T_c in the region of $30 < T < 50\,^{\circ}\mathrm{C}$, all grains regardless of their size have low specific conductivity of $\sigma \approx 10^{-6}$ S/m, and the resonance maximum of the function $\varepsilon''(f)$ corresponding to them is a peak with amplitude and narrow frequency band, i.e. all the grains of the film VO_2 are characterized by only one „monoclinic“, i.e., semiconductor, structural component with a low resonance frequency ($< 10^4$ Hz).

As the temperature increases from 30 to $50\,^{\circ}\mathrm{C}$, the concentration of free electrons increases in all grains of the film, their specific conductivity increases, and the resonance maximum $\varepsilon''(f)$, remaining high in amplitude and narrow in frequency, shifts toward high frequencies. The generation of free electrons into the conduction band of the semiconductor phase VO_2 (temperature extended electronic Mott PT takes place) accelerates with further temperature increase as well as the temperature destabilization of $V-V$-dimers in the crystal lattice [8]. At the beginning of this process, the electronic transition at $T > T_c + \Delta T$ stimulates a structural transition from the monoclinic phase to the tetragonal phase (structural Peierls PT), with only a few percent of the total population of the grains of VO_2 film. We would like to remind that ΔT (a departure from T_c according to the martensitic ideology) is inversely proportional to the square root of the average grain cross-section. For this portion of the grains, the specific conductivity of the material jumps up by about an order of magnitude: from a value of $\sigma \approx 10^{-5}$ S/m to $\sigma \approx 10^{-4}$ S/m. This manifests itself in the fact that the „tetragonal“ component of the spectrum additionally appears at a higher frequency ($f \sim 10^6$ Hz) in the DS, along with the „monoclinic“ component of the DS. The two resonance maxima of the function $\varepsilon''(f)$ corresponding to both components of the DS appear to be reduced in amplitude and broadened in the frequency interval occupied by it, which is manifested in the spectra in the form of the appearance of a thin doublet structure, which was first observed in this work in the course of a detailed study of the PT process with the minimum possible temperature step. The number of grains with tetragonal symmetry of the crystal lattice increases in the temperature region of $60-70\,^{\circ}\mathrm{C}$, which is accompanied by „pumping“ of the intensity of DS singularities from their monoclinic component to the tetragonal one. Only the second „tetragonal“ component (with the maximum frequency of 10^7 Hz) remains in DS at $70\,^{\circ}\mathrm{C}$, and the single resonance maximum $\varepsilon''(f)$ corresponding to it again becomes high in amplitude and narrow in the occupied frequency band, losing its fine structure. The resonant frequency corresponding to it, starting from $T > 70\,^{\circ}\mathrm{C}$, continues to increase up to $100\,^{\circ}\mathrm{C}$.

Thus, at temperatures higher than the PT temperature in the smallest cross-sectional nanocrystallites of VO_2 film, i.e. in the interval of $80 < T < 100\,^{\circ}\mathrm{C}$, the crystal lattice of all grains of the film acquires tetragonal symmetry, and all grains, regardless of their size, acquire high specific conductivity $\sigma > 2 \cdot 10^{-3}$ S/m, the resonance maximum function $\varepsilon''(f)$ again, as in the case of monoclinic lattice symmetry of the semiconductor phase, appears as a high and narrow peak, devoid of fine structure, i.e. it is characterized by only one exclusively „tetragonal“ component with a high resonance frequency ($> 10^7$ Hz).

When the temperature decreases, the movement along the cooling branch of the thermal hysteresis loop in all grains of the film decreases the concentration of free electrons, their specific conductivity decreases, and the resonance features, remaining high in amplitude and narrow in frequency, shift toward low frequencies. All processes in such a motion are repeated in reverse order, and the fine structure of DS is also observed, but at lower temperatures compared to the motion along the heating branch of the hysteresis loop. The

point is that the electronic transition stimulates the structural PT at $T < T_c - \Delta T$, so the cooling branch of the hysteresis loop appears to be shifted towards low temperatures by an amount $2 \cdot \Delta T$ (in our case $\Delta T = 5\,^{\circ}\mathrm{C}$).

Thus, a separate observation of the processes of the Mott electronic transition and the structural Peierls transition in nanocrystallites of VO_2 film has been realized in this study owing to the unique capabilities of the dielectric spectroscopy method, and the magnitude of the change in the specific conductivity of the film in case of the Mott PT (more than 3 orders of magnitude) and Peierls PT (about 1 orders of magnitude) was numerically estimated.

Conflict of interest

The authors declare no conflict of interest.

References

[1] W. Bruckner, H. Opperman, W. Reichelt, E.I. Terukov, F.A. Tschudnovskii. Vanadiumdioxide. Akademie-Verlag, Berlin (1983). 252 p.
[2] N.F. Mott. Perekhody metall-izolyator. Nauka, M. (1979). (in Russian).
[3] V.F. Gantmacher. Elektrony v neuporyadochennykh sredakh. Fizmatlit, M. (2013). p. 288 (in Russian).
[4] A.B. Migdal. UFN **147**, *10*, 210 (1985). (in Russian).
[5] E.B. Shadrin, A.V. Ilyinsky. FTT **42**, *6*, 1092 (2000). (in Russian).
[6] A.V. Ilinskiy, O.E. Kvashenkina, E.B. Shadrin. FTP **45**, 9 (2011). (in Russian).
[7] A.V. Ilinskiy, O.E. Kvashenkina, E.B. Shadrin. FTP, **46**, 9 (2012). (in Russian).
[8] A.V. Ilinskiy, O.E. Kvashenkina, E.B. Shadrin. FTP **46**, 4 (2012). (in Russian).
[9] A. Cavalleri, Cs. Toth, C.W. Siders, J.A. Squier, F. Raksi, P. Forget, J.C. Kieffer. Phys. Rev. Lett. **87**, 237401−1 (2001).
[10] V.G. Golubev, V.Y. Davydov, N.F. Kartenko, D.A. Kurdyukov, A.V. Medvedev, A.B. Pevtsov, A.V. Scherbakov, E.B. Shadrin. Appl. Phys. Lett. **79** (14), 2127 (2001).
[11] A.V. Akimov, A.V. Virchenko, V.G. Golubev, A.A. Kaplyansky, D.A. Kurdyukov, A.B. Pevtsov, A.V. Scherbakov. FTT **45**, *2*, 231 (2003).
[12] A.V. Ilinsky, Ya.O. Veniaminova, R.A. Castro, V.A. Klimov, A.A. Kononov, E.B. Shadrin. FTT **67**, *2*, 391 (2025). (in Russian).
[13] A.V. Ilinskiy, R.A. Kastro, M.E. Pashkevich, E.B. Shadrin. ZhTF **89**, *12*, 1885 (2019). (in Russian).
[14] A.V. Ilinskiy, R.A. Kastro, M.E. Pashkevich, E.B. Shadrin. FTP **54**, *4*, 331 (2020). (in Russian).
[15] S. Havriliak, S. Negami. J. Polym. Sci. C **14**, 99 (1966).
[16] M. Gatti, F. Bruneval, V. Olevano, L. Reining. Phys. Rev. Lett. **99**, 266402 (2007).
[17] A.L. Roitburd. UFN **113**, *69*, 104 (1974). (in Russian).

Translated by A.Akhtyamov